STRAY LIGHT ANALYSIS AND CONTROL
ERIC C. FEST
SPIE PRESS
2013

Chapter 9
Baffle and Cold Shield Design

Baffles and vanes are usually used to block low-order stray light paths and are often the primary means of controlling stray light in an optical system. *Baffles* are cylindrical or conical shaped tubes used to enclose a system or block zeroth-order stray light paths, and *vanes* are structures that go on baffles to block scattering from them. Baffles are generally used to block light from sources well outside the nominal FOV of the system and should be designed to not vignette.[9] They can be difficult to fabricate and add cost and weight to the system; however, they are essential in some systems to ensure proper functioning. An example of such a system is the baseline Maksutov–Cassegrain telescope (shown in Fig. 1.5), which has three baffles:

- A large cylindrical baffle around the primary mirror to prevent direct illumination of the primary. Such a baffle is often called the *main* baffle.[10]
- A baffle in the center of the primary mirror and another around the secondary mirror. These baffles block the zeroth-order external stray path through the hole in the primary mirror. A ray trace of this path is shown in Fig. 3.8.

Another example of a baffle is the cylindrical cold shield around the detector in the LWIR camera shown in Fig. 3.11. This baffle (which was discussed in Chapters 8.3 and 8.4) blocks the zeroth-order internal stray light path from self-emission of the housing around the detector.

The design of any of these baffles should be performed as early in the optical design process as possible, as their size and placement can significantly affect both the optical performance (e.g., vignetting and stray light) and the mechanical characteristics (e.g., size and weight) of the system. This chapter discusses how baffles and vanes can be used to improve system stray light performance, and is divided into the following sections:

- Section 9.1 discusses a method to determine the optimal length and diameter of the main baffle.
- Section 9.2 discusses methods to determine the optimal size and placement of baffle vanes.
- Section 9.3 discusses the design of the primary and secondary mirror baffles in the baseline Maksutov–Cassegrain system.

- Section 9.4 discusses some nontraditional vane designs to utilize highly specular, nonplanar surfaces. These baffles are usually more difficult to fabricate than traditional planar baffles but can perform better in some applications.
- Section 9.5 discusses the design of masks and dimples to prevent stray light paths from unused portions of the optics, such as the unused portion of the secondary mirror in Cassegrain-type systems.

The methodologies presented in this chapter can be applied to the design of baffles of any type of optical system, even those not specifically considered here.

9.1 Design of the Main Baffles and Cold Shields

Main baffles, such as the one shown in Fig. 9.1, are common in optics and are used to shadow (i.e., prevent direct illumination of) an optical element or the focal plane. The baseline Maksutov–Cassegrain telescope has a main baffle (which, when used on a telescope, is sometimes called the *telescope barrel*) that also serves as a mounting structure for the corrector lens and is often used in a similar way for other centrally obscured systems. Commercial camera lenses (such as the one shown in Fig. 9.2) also often have main baffles, which are sometimes called *lens hoods*. The element that is shadowed is referred to generically in this book as the *collector*. In the baseline Maksutov–Cassegrain telescope, the collector is the primary mirror. In the camera in Fig. 9.2, the collector is the first element of the zoom lens.

The length L and diameter D of the main baffle, and the diameter d of the collector determine the minimum angle of a collimated off-axis source θ_{min} at which

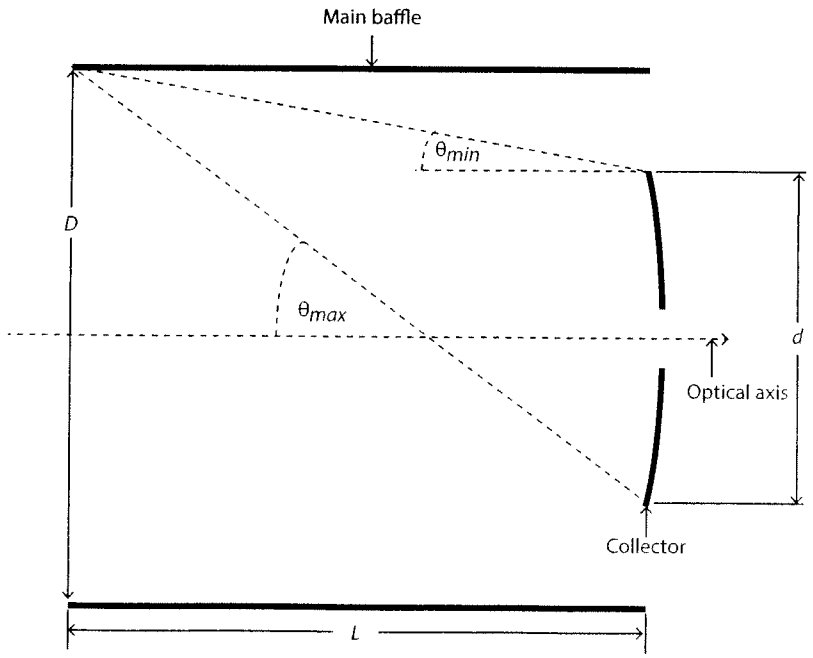

Figure 9.1 Main baffle length and diameter.

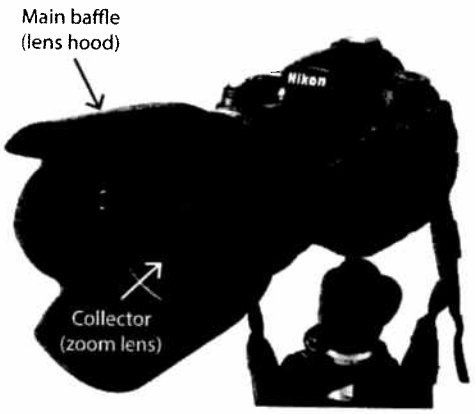

Figure 9.2 A main baffle (lens hood) and collector (zoom lens) on a commercial camera lens. The lens hood has notches in it to prevent vignetting at the corners of the FOV.

the collector is no longer directly illuminated. θ_{min} is given by

$$\theta_{min} = \tan^{-1}\left(\frac{D-d}{2L}\right), \tag{9.1}$$

and θ_{max} is given by

$$\theta_{max} = \tan^{-1}\left(\frac{D+d}{2L}\right). \tag{9.2}$$

These quantities are shown in Fig. 9.1.

To the first order, the effect of the main baffle on the PST of this system can be determined by computing the percent overlap in the projected area of the main baffle entrance aperture and the collector, as shown in Fig. 9.3. This PST is often called the *shadow function* of the baffle because it determines the amount that the collector is shadowed. The shadow function is equal to unity (i.e., no shadowing)

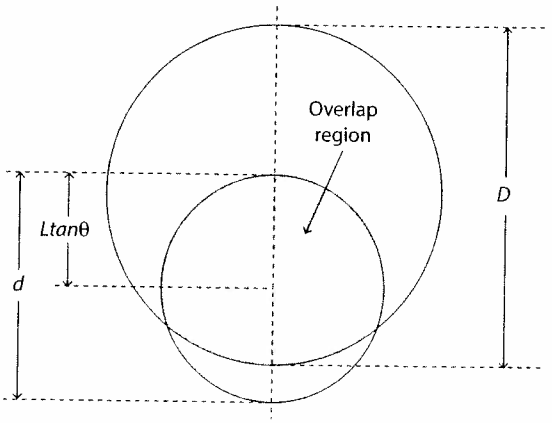

Figure 9.3 Geometry used for baffle shadow function calculation. The dimensions refer to those shown in Fig. 9.1.

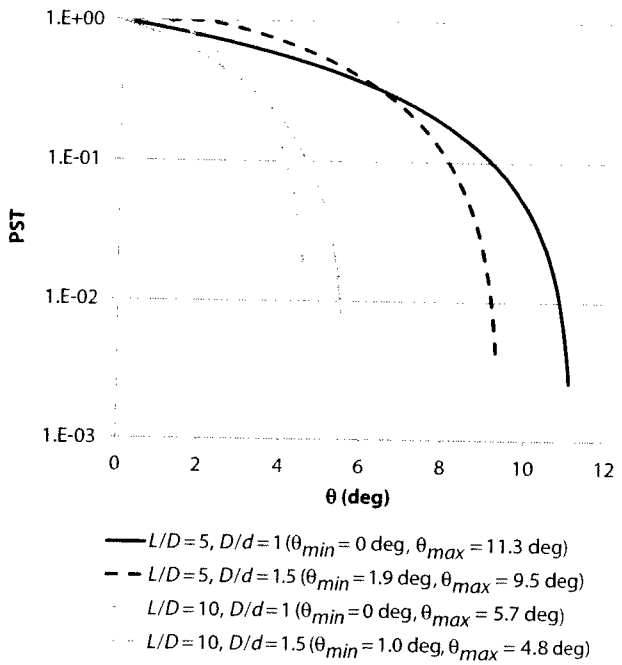

Figure 9.4 PST at the collector versus angle of a collimated source from optical axis θ for different baffle geometries. The dimensions refer to those in Fig. 9.1.

for source angles less than or equal to θ_{min}, and the baffle is often designed such that θ_{min} is equal to half of the system FOV, as it is usually not desirable to shadow (or vignette) the FOV. In systems with small FOVs, setting θ_{min} equal to half the FOV may not be practical, as it may result in a very long main baffle. The shadow function is equal to zero (i.e., totally shadowed) for source angles greater than or equal to θ_{max}, and the baffle is often designed such that θ_{max} is equal to the exclusion angle, which is often a part of the stray light requirement for the system and defines the minimum angle at which the stray light requirement must be met (see Section 2.2.3). θ_{min}, θ_{max}, and PST for different values of L/D and D/d are shown in Fig. 9.4. In the case where the $D = d$, the shadow function PST is given by[10]

$$PST = 1 - \frac{1}{4}\left|5\left(1 - \left|\frac{\theta}{\theta_{max}}\right|\right) - 1 + \left(\frac{\theta}{\theta_{max}}\right)\right| \tag{9.3}$$

if $|\theta/\theta_{max}| \leq 1$, and zero otherwise.

Figure 9.4 shows that the larger the value of D/d, the larger the value of θ_{min}, which suggests that systems with large FOVs must have a main baffle much wider than the primary (i.e., a large D) to prevent vignetting. In practice, this increase in size may be prohibitive, and therefore some systems have $D/d = 1$ and accept the vignetting that occurs.

Figure 9.4 also shows that the larger the value of L/D, the smaller the value of θ_{max}, which suggests that longer main baffles can block light from off-axis sources closer to the edge of the FOV. Although it is desirable, from a stray light

Figure 9.5 Sugar-scoop baffle on the Infrared Astronomical Satellite.[12]

performance standpoint, to make θ_{max} as close to the edge of the FOV as possible, in practice this is often impractical because it results in a very long and heavy main baffle. In some cases, a portion of the main baffle might not be illuminated, either as a natural consequence of the illumination geometry or by controlling the orientation of the sensor relative to the illumination. In these cases, the weight of the baffle can be reduced by removing the portion of it that is never illuminated. Such a baffle is sometimes called a *sugar-scoop baffle* and was used on the Infrared Astronomical Satellite (IRAS), as shown in Fig. 9.5.

The simplistic calculation of the PST from the shadow function shown in Fig. 9.4 neglects the effect of scatter from the inner diameter (ID) of the baffle, which is discussed in the next chapter.

9.2 Design of Vanes for Main Baffles and Cold Shields

The ID of the main baffle is often both illuminated and critical as seen from the collector, and will therefore scatter directly to it. The radius of the main baffle can create a caustic in the reflected beam and thus create regions of high irradiance

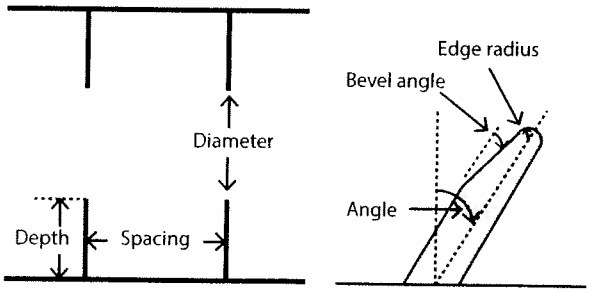

Figure 9.6 Illustration of the baffle vane parameters in Table 9.1.

Table 9.1 Design parameters for baffle vanes.

Vane Parameter	Definition
Aperture	Diameter of the hole in the vane
Depth	Distance from the tip of the vane to the ID of the main baffle
Spacing	Distance between adjacent vanes
Edge radius	Radius of curvature of edge of vane aperture
Bevel angle	Angle of bevel relative to vane surface
Angle	Angle relative to main baffle
Coating	Type of paint or treatment

on the collector, especially if the surface treatment of the ID is specular. These reflections can be blocked using vanes (apertures within the main baffle). The design variables for vanes are given in Table 9.1.

The goal in baffle vane design is typically to block all first-order stray light paths off of the ID of the main baffle and to not vignette the FOV of the collector.

9.2.1 Optimal aperture diameter, depth, and spacing for baffle vanes

The goal in baffle vane design is typically to block all first-order stray light paths off of the ID of the main baffle and to not vignette the FOV of the collector. An example of a vane design (for the cold shield for the LWIR camera shown in Fig. 3.11) is shown in Fig. 9.7.

The initial design consists of only the entrance aperture, main baffle, and collector. The entrance aperture diameter is usually determined by the FOV and/or the $f/\#$ of the system. The diameter of the collector used in baffle vane design is always its maximum diameter; in most cases, this diameter will be the diagonal of the primary mirror (i.e. the critical portion) or of the detector.

The dotted lines in Fig. 9.7(a) are construction lines used to determine the baffle vane depth, spacing, and bevel angles. Approximate solutions to these lines can be done graphically using a drawing program or exactly using linear equations, which is the recommended method and is used here. The numbers in Fig. 9.7 refer to the steps used in constructing the design:

1. Draw a ray between the $+y$ edge of the entrance aperture and the $+y$ edge of the collector. This ray defines a "keep-out" zone that prevents the FOV of collector from being vignetted.
2. Draw a ray from the $-y$ edge of the critical portion of the collector to the $+y$ corner of the main baffle.
3. Place a baffle at the intersection point between the rays from step 1 and step 2.

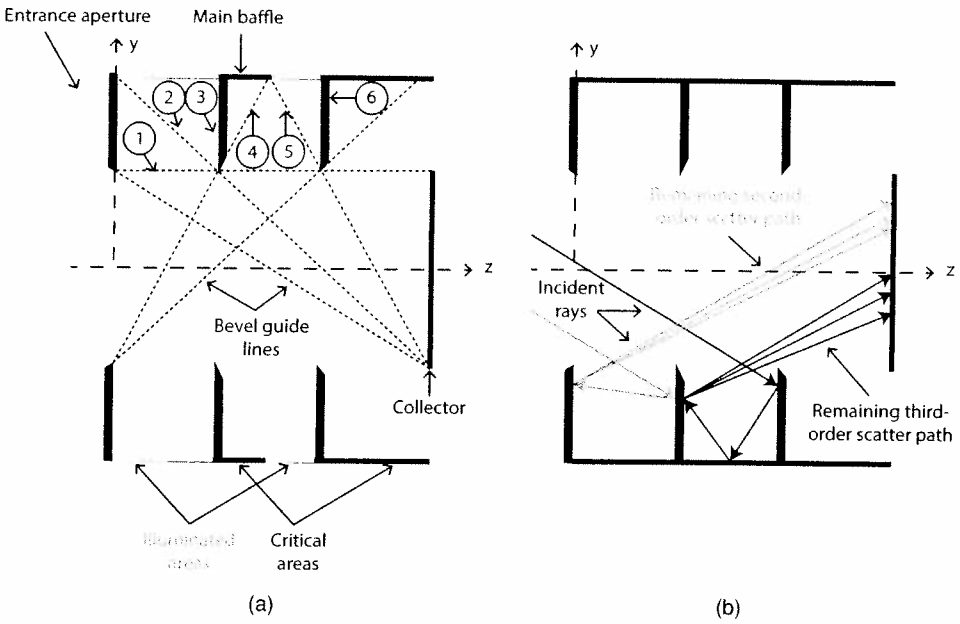

Figure 9.7 (a) Steps in a diffuse baffle vane design for a cold shield, and (b) examples of remaining higher-order paths. Figures are not to scale.

4. Draw a ray from the $-y$ edge of the entrance aperture to the $+y$ edge of the second baffle vane aperture.
5. Draw a ray from the intersection point between the ray from step 4 and the main baffle to the $-y$ edge of the critical portion of the collector.
6. Place a baffle at the intersection point between the ray from step 1 and the ray from step 5.

Repeat steps 4–6 as many times as necessary, until the end of the main baffle is reached. Figure 9.7(a) shows that this baffle design works by preventing adjacent portions of the ID of the main baffle from being both critical and illuminated, as seen from the collector. The only paths that remain are higher-order ones, as illustrated in Fig. 9.7(b). The number of baffle vanes should not be allowed to get so large that the magnitude of scattering from the edges of the vanes exceeds that of the scattering from the ID of the main baffle without vanes. The maximum diameter of the baffle vane apertures are computed using the maximum dimension of the critical portion of the collector; however, the vane apertures may need to be smaller in other cross-sections because the "keep-out" zone is smaller. In general, increasing the depth of the vanes beyond the depth computed using the algorithm shown in Fig. 9.7 does little to improve the stray light performance of the system. If knife-edges and bevels are to be used on the vane tips, the bevel angles should be chosen to prevent the bevels from being both illuminated and critical, as shown in Fig. 9.7. This issue is discussed in more detail in Section 9.2.2.

Figure 9.8 shows an out-of-plane view of the cold shield designed in Fig. 9.7. Because the entrance aperture is circular and the collector is square, the optimal

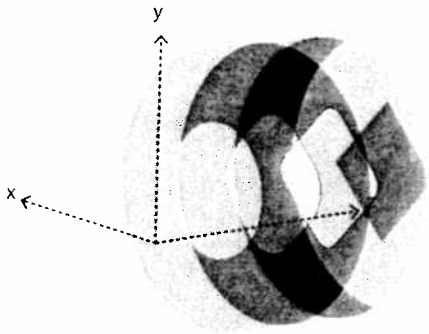

Figure 9.8 Out-of-plane view of the cold shield designed in Fig. 9.7. The diagonal of the detector is along the *y* axis. The model was created in FRED.

aperture shapes are "racetracks," or squares with rounded corners (also called "squircles"). The radii of these corners are approximately equal to $(D/2) \times (1 - z/L)$, where D is the diameter of the circular entrance aperture, z is the axial distance between the vane and the entrance aperture, and L is the distance between the entrance aperture and the collector. Table 9.2 gives the dimensions of baffle and vanes.

One way of quantifying the performance of this design is to compute its *cold shield efficiency* η, which is defined as

$$\eta = \frac{E_{direct}}{E_{direct} + E_{indirect}}, \tag{9.4}$$

where E_{direct} is the irradiance on the detector that comes directly from a uniform, Lambertian scene; and $E_{indirect}$ is the irradiance on the detector that comes from scattering and all other stray light mechanisms within the cold shield cavity. The quantity is similar to the VGI defined in Eq. (2.44). The efficiency of this cold shield is computed by entering the design into FRED and performing a backwards ray trace to the entrance (cold stop) aperture, and allowing rays from the ID and from the vanes to scatter directly or indirectly to the aperture. The Aeroglaze® Z306 BRDF

Table 9.2 Dimensions of the apertures in the cold shield design shown in Fig. 9.8. The ID of the main baffle cylinder is 12 mm.

Aperture	z Location (mm)	Semi-Width (mm)	Racetrack Corner Radius (mm)
Cold stop	0.0000	2.9289	2.9289
Vane #1	3.2666	2.6094	1.7120
Vane #2	6.5341	2.3708	0.8029
Detector	9.7649	2.1596	0.0000

Table 9.3 Cold shield efficiency with and without baffle vanes. The cold shield geometry is shown in Fig. 9.8. The inside of the cold shield is painted with Aeroglaze® Z306, and the analysis is performed at 10.6 μm.

Configuration	Efficiency (fractional)
w/o baffle vanes	0.9758
w/ baffle vanes	0.9999

model at 10.6 μm given in Chapter 6 is used to model the scattering properties of the black surface treatment. The results are shown in Table 9.3. The addition of the baffle vanes reduces all first-order scatter paths and raises the efficiency about 0.02, giving it near-perfect efficiency. This analysis neglects scattering from the vane edges, which will decrease efficiency.

Cold shield efficiency is usually the best way to quantify the effectiveness of the baffle vane design for cold shield. However, for other applications, such as controlling solar stray light in the main baffle of a telescope, it is useful to show the PST of the baffle with and without vanes (Fig. 9.9). The PST is computed as the irradiance on the collector divided by the irradiance at the entrance aperture. As expected, adding the vanes significantly reduces the PST, by as much as a factor of 1900. This analysis also neglects the effect of reflections from the edges of the vane apertures.

For some vane geometries, specular black paints may yield better stray light performance.[11]

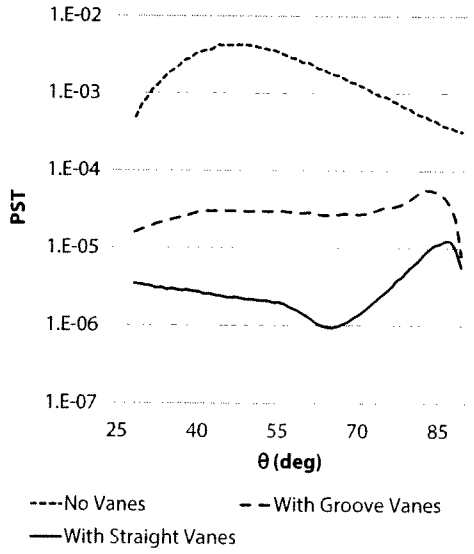

Figure 9.9 PST of the baffle design shown in Fig. 9.8 for three configurations: with no vanes, with groove vanes, and with straight vanes (see Section 9.2.3).

9.2.2 Edge radius, bevel angle, and angle for baffle vanes

Because the edges of the baffle vanes can scatter directly to the collector, their edge radii should be made as small as possible. This is usually done by adding a bevel to the baffle vanes and by making the edge a knife edge, as shown in Fig. 9.6. The smallest edge radius that can be easily made is typically about 0.005″ (0.127 mm). Care must be used when applying paint to these edges because it can increase their radius, which increases their projected solid angle and the amount of light they scatter to the collector. Paint can also be easily chipped off of these edges, which can increase their BRDF. The effect of edge scatter on stray light performance can be evaluated in stray light analysis software by adding the edges to the model. This analysis is especially important to do in baffle designs with many vanes, as scattering from the edges may result in a system with more stray light than a system with fewer vanes.

The bevel angle for each vane should be chosen so that the bevel is not both critical and illuminated, as shown in Fig. 9.7(a). Because the bevel on the entrance aperture is likely to be illuminated, it should face outward so that it is not critical. The bevels on the other vanes should face inward so that they are not illuminated, as doing so increases the angle between the scattered and specular rays in the first reflection of higher-order scatter paths to the collector, such as the ones shown in Fig. 9.7(b). Increasing this angle generally decreases the BRDF and therefore reduces the flux in these paths.

The bevels shown in Fig. 9.7 were designed assuming that the bevel angle can be different for each vane. However, the vanes may be easier to fabricate if the bevel angle is constant. In this case, it is possible to prevent the bevels from being both critical and illuminated by orienting them as shown in Fig. 9.10.[2] In order to prevent their bevels from being critical, vanes near the entrance aperture of the main baffle should be oriented so that their bevels face outward. The opposite should be done for vanes near the collector: their bevels should be oriented facing inward, to prevent them from being illuminated. The distance z_0 from the entrance aperture at which the orientation of the bevels should switch is equal to $[-D \times L + L \times \sqrt{(d \times D)}]/(d - D)$, where d, D, and L are those variables shown in Fig. 9.1. This design requires that the bevel angle be less than $\arctan\{z_0/[D + (d - D) \times z_0/(2 \times L)]\}$.

Using a nonzero baffle vane angle (such as the one shown in Fig. 9.6) typically does little to improve stray light performance.[2] Such baffles are much more difficult to fabricate and are therefore rarely used.

9.2.3 Groove-shaped baffle vanes

In some cases, groove-shaped vanes (such as the ones shown in Fig. 9.11) may be easier to fabricate than the straight vanes shown in Fig. 9.7. For instance, groove-shaped vanes may be easier to lathe into the ID of a lens barrel because they are a continuous surface, whereas straight vanes are not. This is especially true in systems with tight space constraints and with a large number of vanes.

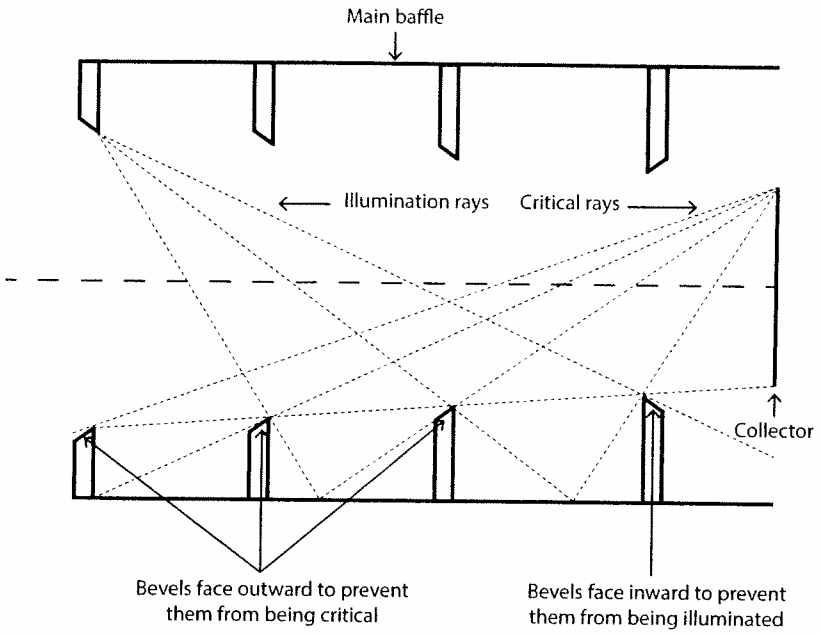

Figure 9.10 Optimal vane bevel orientation for vanes with constant bevel angles.

The rules for designing groove-shaped vanes are the same as those for designing straight vanes: the design should prevent overlap between critical and illuminated areas. This rule was used to design optimal groove-shaped vanes for the cold shield considered earlier; the resulting design is shown in Fig. 9.11. The steps used to generate this design are similar to the steps used to generate the straight-vane design. A tighter space constraint was used on the groove-vane design; the

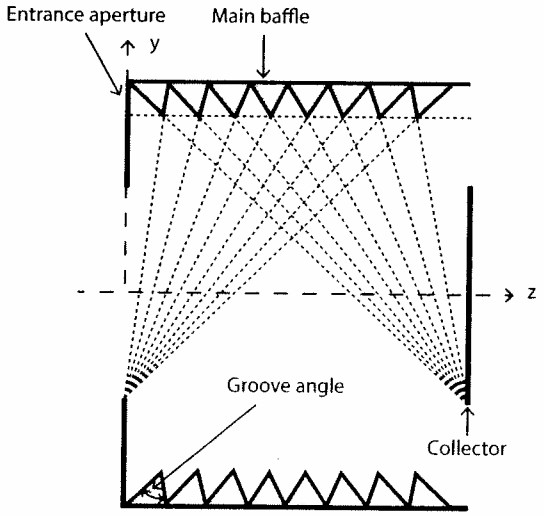

Figure 9.11 Groove-shaped vane design for the cold shield shown in Fig. 9.7. Figure is not to scale.

minimum ID of the vanes was larger than that of the straight vane design. This was done so that the performance of groove vanes in a system with tight space constraints could be demonstrated. The PST of the groove vane design is shown in Fig. 9.9. This PST calculation was performed assuming that same paint applied to the straight vanes (Aeroglaze® Z306 at 10.6 μm) was also applied to the groove vanes.

As the figure shows, the groove-vane design does not perform as well as the straight-vane design, which is because the vane cavities are shallower in the grooved design (because there are more of them) and because groove vanes are not as efficient at trapping light as straight vanes; as a result, there is more flux in the second-order stray light paths in the grooved design than in the straight design. For this reason, groove-vane designs generally do not perform as well as straight-vane designs with the same depth and spacing. Groove vanes may also be fabricated with constant groove angles, which may make them easier to fabricate but will also degrade their performance relative to optimal groove vane designs, such as the one shown in Fig. 9.11.

9.3 Design of Baffles for Cassegrain-Type Systems

Optimal baffle designs for Cassegrain-type systems block the zeroth-order path to the focal plane (shown in Fig. 3.8) while minimizing vignetting by the primary and secondary mirror baffles. An example of an artifact that results from this path is shown in Fig. 1.2. This artifact is created by shortening the primary mirror baffle in the baseline Maksutov–Cassegrain telescope and then taking a photograph of a featureless scene with the sun just outside the FOV. The sun directly illuminates the detector via the path shown in the ray trace in Fig. 3.8. The primary mirror baffle is shortened in the stray light model, and the artifact is reproduced in Fig. 9.12.

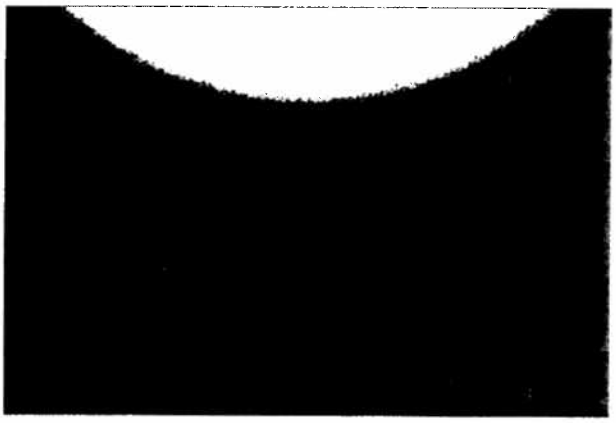

Figure 9.12 The stray light artifact due to the zeroth-order path in the modified Maksutov–Cassegrain telescope. The telescope was modified by shortening the primary mirror baffle by about 1″. The sun is at 10 deg from the optical axis, just outside the lower edge of the FOV. This artifact is very similar to the artifact observed in the as-built system shown in Fig. 1.2.

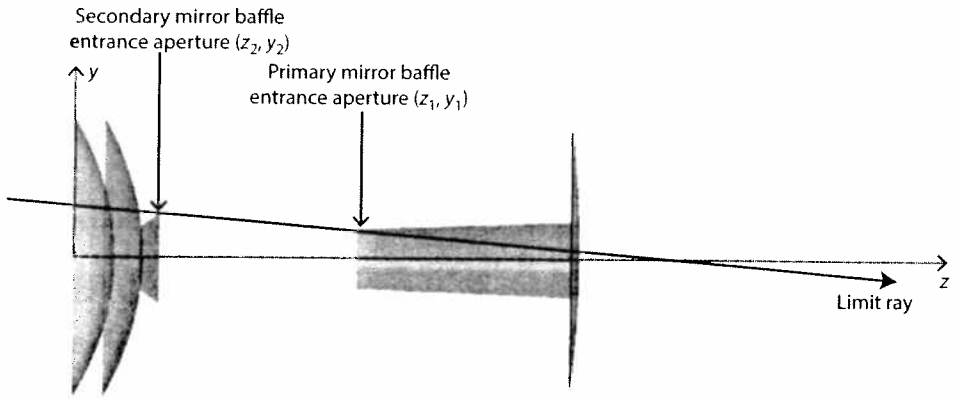

Figure 9.13 The baffles in the baseline Maksutov–Cassegrain system. The limit ray goes through the tips of the primary and secondary mirror baffles to the edge of the detector.

The size of the baffles for Cassegrain systems with spherical primaries and secondaries can be computed using closed-form solutions.[3] For other systems, the baffle sizes can be computed using the optimizer in a stray light analysis program. Figure 9.13 shows the four variables that must be optimized: the axial locations and semidiameters of the primary and secondary mirror baffle entrance apertures (z_1, y_1 and z_2, y_2, respectively).

The merit function should be computed as the weighted sum of the following quantities:

1. The flux that leaves the system through the entrance aperture via the zeroth-order path from a backward ray tracing source on the focal plane. The source must fill the image and should be collected on a surface at the telescope entrance aperture. The merit function should be heavily weighted by this flux, as the goal is to eliminate this flux completely.
2. The flux vignetted by the baffles from forward ray tracing sources at the center and corner field points.

Optimizing the baffles in this way eliminates the zeroth-order path and minimizes the amount of vignetting. This method is used to compute the size of the baffles for the baseline Makstuov–Cassegrain system, and the resulting sizes closely match those in the as-built system. The baffles are shown in Fig. 9.13. In this design, the main baffle does not block the zeroth order path to the detector, because it is too short and the detector is too small. However, if the main baffle is long enough, it can help block the path, and the optimal primary and secondary mirror baffles will vignette less than they would without it. If the θ_{min} of the main baffle [as defined in Eq. (9.2)] is equal to half of the system FOV, then it will completely block the zeroth-order path, and no primary and secondary mirror baffles are necessary; this is usually impractical, as it requires the main baffle to be very long.

In optimal (or nearly optimal) baffle designs, the tip of the secondary mirror baffle, the tip of the primary mirror baffle, and the edge focal plane all lie on the

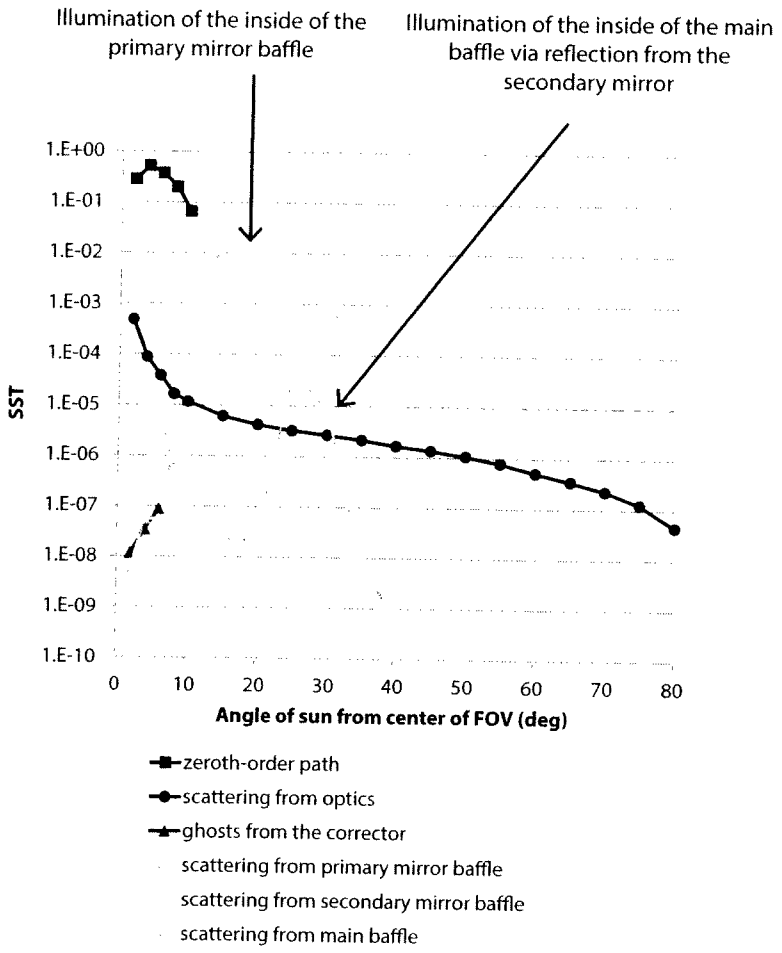

Figure 9.14 SST of elements in the baseline Maksutov–Cassegrain system, as predicted by the FRED model.

same limit ray, as shown in Fig. 9.13. This design ensures that the baffles are as small as possible while ensuring that the zeroth-order path is blocked.

The SST predicted by the FRED model from each element in the system is shown in Fig. 9.14, and the total SST of the system with and without baffles is shown in Fig. 9.15.

A number of conclusions can be drawn from Fig. 9.15:

- As expected, blocking the zeroth-order path with the baffles greatly reduces the SST at small angles.
- Adding baffles increases the SST at larger angles because they are illuminated and can scatter directly to the detector. The peak at about 15 deg in the SST of the primary mirror baffle is due to scattering from the inner diameter of the primary mirror baffle, as shown in Fig. 9.16. This path raises the SST significantly because the scattering from the inside of the baffle is near specular. This path can be reduced by adding vanes to the inside of

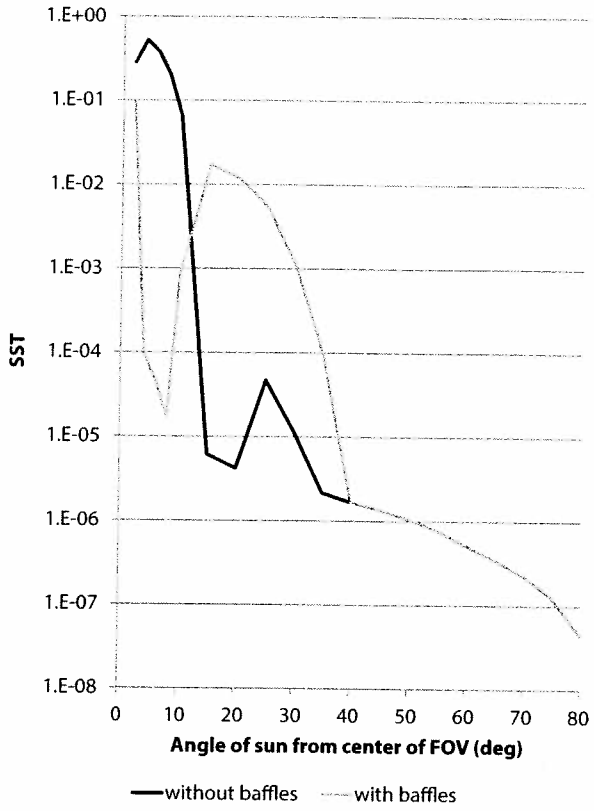

Figure 9.15 SST of the entire baseline Maksutov–Cassegrain system, with and without baffles, as predicted by the FRED model.

the baffle, by lowering its BRDF, or by shadowing the baffle with a larger secondary baffle and/or longer main baffle. It can also be eliminated by adding a field stop or by making the aperture stop the last element in the system before the focal plane, as discussed in Section 8.3.

- The overviewing path off of the ID of the main baffle that occurs at 25 deg (illustrated in Fig. 3.9) is not a concern in this system because its flux is much

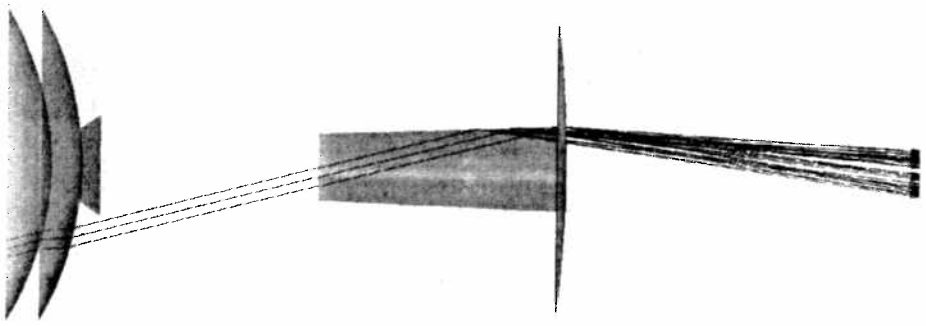

Figure 9.16 Near-specular scattering from the inside of the primary mirror baffle due to illumination by the sun at 15 deg from the center of the FOV.

less than the flux of the path off of the ID of the primary mirror baffle. This is not the case in a system without a primary mirror baffle, as shown in Fig. 9.15. The magnitude of this path could be reduced by adding vanes to the ID of the main baffle or by lowering its BRDF. It could be eliminated by making the main baffle longer or by moving the aperture stop from the primary to an element deeper in the system, as discussed in Section 8.3.

- Ghosts from the corrector occur only at small angles, which is typical of ghost reflection paths.
- Most stray light at high angles is due to scattering from the corrector. This can be reduced by shadowing the corrector with a baffle or by reducing the corrector's surface roughness or particulate contaminants.

Comparison between the predicted and measured SST is presented in Section 11.4; the predicted matches the measured to within a factor of 5. Agreement to within a factor of two is considered very good, as the agreement between the predicted and measured BSDF of a single optical surface is often not better than this (as discussed in Sections 4.1.3 and 5.3.4). As expected, the first-order model does not predict scattering from the baffles.

9.4 Design of Reflective Baffle Vanes

A number of baffle vane designs have been developed that reflect incident light back out the entrance aperture of system.[4] Unlike the vanes discussed previously in this chapter, these vanes have high reflectance, on the order of 0.9 or higher. These vanes have a number of advantages: they have low emissivity (and therefore may have better internal stray light performance than highly absorbing baffles and do not heat up as much), can generate less particulate and molecular contamination, and may perform better over systems with large wavebands. However, they also have a number of drawbacks, including that they can have worse external stray light performance than comparable absorbing baffles, they can be difficult and expensive to fabricate, and can be heavier than standard vanes; therefore, they may be suitable for some but not all applications.

An ellipsoidal baffle vane design[5] is shown in Fig. 9.17. Each vane is a section of an ellipse that has one focus at the edge of the vane in front of it and another at the edge of the entrance aperture. This arrangement ensures that all of the rays that lie in the plane of the ellipse will be rejected out the entrance aperture. Unfortunately, some skew rays (about 10%) will not be rejected, and therefore the back sides of the baffle vanes need a black surface treatment. The vanes must be positioned so that no entering rays can strike the inner diameter of the main baffle.

Another design, patented by Lockheed,[7] is designed using alternating confocal ellipses and hyperbolas, as shown in Fig. 9.18. The focusing properties of these conic sections are such that any in-plane ray that enters between the two foci must, after one or more reflections, be rejected between the foci. Analysis indicates that the same is true for all skew rays.

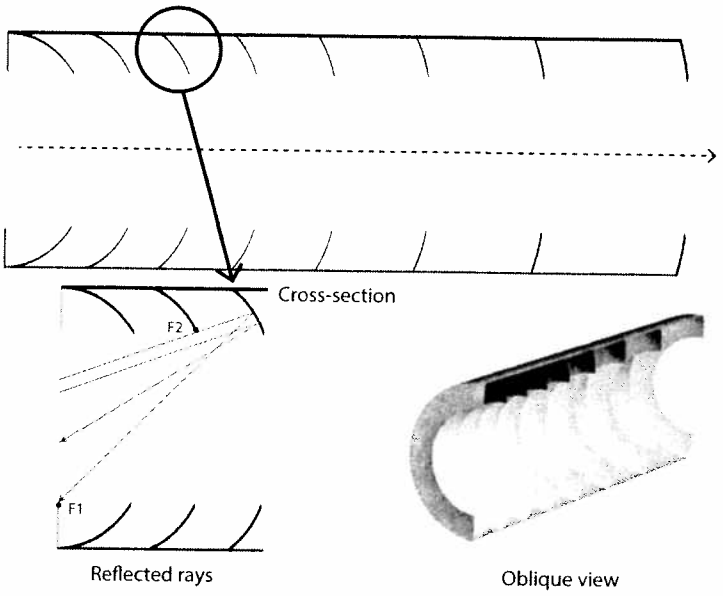

Figure 9.17 Elliptical baffle vanes. All in-plane rays are rejected by the baffle vanes, which have one focus at the edge of the entrance aperture (point F_1) and another at the edge of the vane in front of them (point F_2).

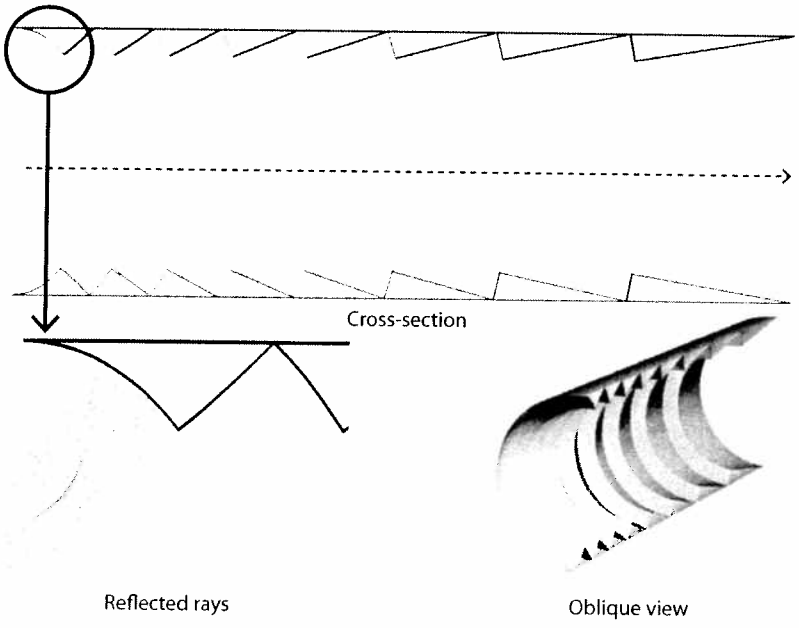

Figure 9.18 Lockheed–Stavroudis baffle vanes, which are composed of alternating confocal ellipses and hyperbolas.

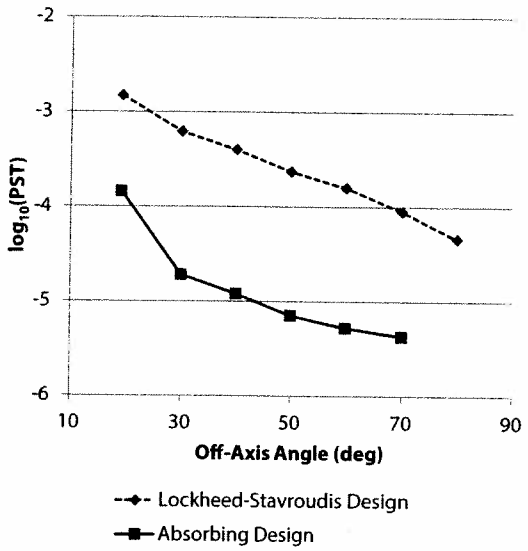

Figure 9.19 PST of the Lockheed–Stavroudis specular baffle vane design and a comparable absorbing baffle vane design. The characteristics of the vane designs are given in Table 9.4.

Figure 9.19 compares the PST of the Lockheed–Stavroudis design shown in Fig. 9.18 to a comparable absorbing baffle design.[4] The characteristics of each design are given in Table 9.4. The Harvey model (discussed in Chapter 4) was used to model the scattering properties of the baffle vanes in each design. In the Lockheed–Stavroudis design, the Harvey model is typical of mirror surfaces, and with a high slope and low TIS (about 0.01). In the absorbing design, the Harvey model is Lambertian with a TIS of 0.06. The PST of the Lockheed-Stavroudis

Table 9.4 Characteristics of the Lockheed–Stavroudis and absorbing baffle vane designs evaluated in Fig. 9.19

	Lockheed-Stavroudis Vane Design	Absorbing Vane Design
Diameter of entrance aperture (in)	4	4
Baffle length (in)	11.6	11.6
Edge radii (in)	0.0039	0.0039
Number of vanes	8	8
Vane depth (in)	0.5	1
Specular reflectance	0.9	0
Slope of Harvey scatter model	−1.5	0
TIS of Harvey scatter model	0.01	0.06

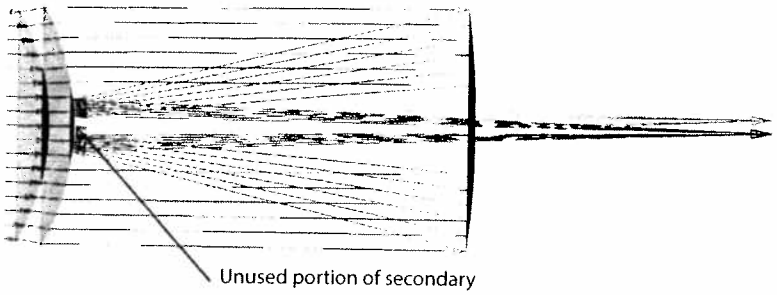

Figure 9.20 The unused portion of the secondary mirror due to the secondary obscuration in the baseline Maksutov–Cassegrain design.

design is higher because it has first-order scatter paths to the detector, whereas the absorbing baffle design does not. This plot demonstrates that the benefits of using a specular baffle vane design must be weighed against poorer external stray light performance.

9.5 Design of Masks

In many optical systems, portions of one or more of the optics are unused, and these unused portions can couple stray light to the focal plane. For instance, the pupil in Cassegrain systems has a hole in its center due to the secondary obscuration, and therefore the center of the secondary mirror is unused, as shown in Fig. 9.20.

External stray light paths that can use this portion of the secondary include reflective ghost paths, such as the one shown in Fig. 7.7. This and other paths can be blocked by applying a black surface treatment (such as paint) to mask off the unused portion of the secondary mirror. Internal stray light paths off of unused areas such as this can be mitigated by using a dimple, as discussed in Section 8.12.

9.6 Summary

Baffles and vanes are usually used to block low-order stray light paths, and as such are often the primary means of controlling stray light in an optical system. Baffles are cylindrical or conical tubes used to enclose a system or block zeroth-order stray light paths, and vanes are structures that go on baffles to block scattering from them. The *main baffle* is a cylindrical baffle usually designed to prevent some element (such as the primary mirror or detector) from being illuminated.

The algorithm shown in Section 9.2.1 can be used to determine the optimal size and position of vanes within a main baffle. The configuration is optimal because it completely prevents the overlap between critical and illuminated areas using the smallest number of vanes. Scattering from the edge of the baffle vanes can be reduced by making the edge radii as small as possible (i.e., using knife edges). Edge scatter can never be eliminated completely, and therefore adding more vanes to the system can sometimes be detrimental to system stray light performance. Bevels on knife-edged vanes should be designed such that they are not both illuminated and

critical. Groove-shaped vanes are often used on the inside diameter of main baffles and lens tubes as a means of reducing stray light; they may be easier to fabricate (but may not perform as well) as straight baffle vanes.

The zeroth-order path through the hole in the primary mirror in Cassegrain-type systems can be blocked using baffles on the primary and secondary mirror. These baffles can be designed for minimum vignetting using the optimization algorithm in stray light analysis software.

Highly reflective baffle designs exist that reflect much of the light incident on the inside of the main baffle back out the entrance aperture. These designs can be advantageous because they may have better internal stray light performance than comparable absorbing baffle vane designs and may not generate as much particulate and molecular contamination. However, they can be difficult to fabricate and may have worse external stray light performance.

Masks can be used on unused areas of optical elements (such as in the center of the secondary mirror) to block stray light paths that use these areas.

References

1. E. Freniere, "First-order design of optical baffles," *Proc. SPIE* **257**, 19–28 (1980) [doi: 10.1117/12.959598].
2. R. Breault, "Vane structure design trade-off and performance analysis," *Proc. SPIE* **967**, 90–117 (1988) [doi: 10.1117/12.948095].
3. W. Hales, "Optimum Cassegrain Baffle Systems," *Appl. Opt.* **31**(25), 5341–5344 (1992).
4. G. Peterson, S. Johnston, and J. Thomas, "Specular baffles," *Proc. SPIE* **1753**, 65–76 (1992) [doi: 10.1117/12.140692].
5. J. Bremer, "Baffle design for earth radiation rejection in the cryogenic limb-scanning interferometer/radiometer," *Proc. SPIE* **245**, 54–62 (1980) [doi: 10.1117/12.959333].
6. W. Linlor, "Baffle System Employing Reflective Surfaces", NASA Technical Memorandum 84406 (1983).
7. O. Stravroudis and L. Foo, "System of reflective telescope baffles," *Opt. Eng.* **33**(3), 675–680 (1994) [doi: 10.1117/12.159338].
8. R. Breault, "Control of Stray Light," in *The Handbook Of Optics, Vol IV*, 3rd Ed., M. Bass, G. Li, and E. Van Stryland, Eds., pp. 7–10, McGraw-Hill, New York (2010).
9. "Stray Light Short Course Notes," Photon Engineering LLC, used with permission (2011).
10. A. Greynolds, "Formulas for estimating stray light levels in well-baffled optical systems," *Proc. SPIE* **257**, 39–49 (1980) [doi: 10.1117/12.959600].
11. E. Freniere, "Use of specular black coatings in well-baffled optical systems," *Proc. SPIE* **675**, 126–133 (1986) [doi: 10.1117/12.939490].